



X International Conference on Structural Dynamics, EURODYN 2017

Asymptotic approximation of the band structure for tetrachiral metamaterials

Marco Lepidi^{a,*}, Andrea Bacigalupo^b

^aDICCA - Università di Genova, Via Montallegro 1, 16154 Genoa, Italy

^bIMT School for Advanced Studies Lucca, Piazza S. Francesco 19, 55100 Lucca, Italy

Abstract

Tetrachiral materials are characterized by a cellular microstructure made by a periodic pattern of stiff rings and flexible ligaments. Their mechanical behaviour can be described by a planar lattice of rigid massive bodies and elastic massless beams. Therefore, the periodic cell dynamics is governed by a monoatomic structural model, conveniently reduced to the only active degrees-of-freedom. The paper presents an explicit parametric description of the Floquet-Bloch spectrum (or band structure) governing the propagation of elastic waves through the tetrachiral material. By virtue of multiparametric perturbation techniques, an analytical asymptotic approximation is achieved for the dispersion surfaces in the Brillouin zone. Since different optimization strategies tend to fail in opening low-frequency band gaps in the material spectrum, this specific design purpose is commonly pursued by introducing interring inertial resonators. The paper demonstrates that multiparametric perturbation methods can efficiently deal with the consequent enlargement of the parameter space, necessary to describe the resulting inertial metamaterial. Indeed, paying due attention to the doubling of internal resonance conditions, an accurate parametric approximations of the enriched band structure can be achieved. From the applicative perspective, the research findings furnish suited analytical tools for the optimal design of pass and stop bands.

© 2017 The Authors. Published by Elsevier Ltd.

Peer-review under responsibility of the organizing committee of EURODYN 2017.

Keywords: Tetrachiral material; inertial metamaterials; wave propagation; perturbation methods; periodic structures.

1. Introduction

Driven by a virtuous synergy with the most recent developments in the parametric design, multi-scale modeling, multi-disciplinary research and computational analysis, cellular and periodic materials are currently encountering a renewed extraordinary success, which overcomes their well-established tradition in the engineering applications. In this respect, advanced theoretical formulations and revolutionary manufacturing technologies offer solid prospects for the birth of new-generation materials with superior mechanical properties and smart multi-field functionalities.

Among the most promising perspectives and challenges within the mechanical compass, the marked anisotropy of some chiral or anti-chiral lattice materials can be exploited to steer or guide elastic waves along particular directions. Furthermore, the periodic microstructure of the irreducible cell can be designed or optimized to govern the dispersion relations of the propagating waves, by properly tuning pass or stop frequency bands in the material spectrum [1–4].

* Corresponding author. E-mail address: marco.lepidi@unige.it

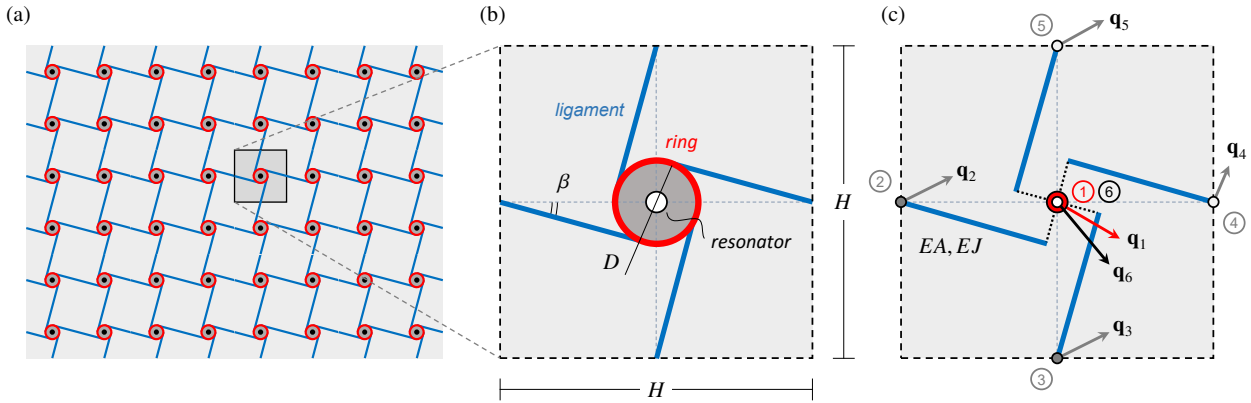


Fig. 1. Tetrachiral metamaterial (a) repetitive planar pattern, (b) periodic cell, (c) beam lattice model.

The present paper illustrates the descriptive power of some asymptotic tools in the parametric sensitivity analysis of the dispersion functions in the whole irreducible Brillouin zone of tetrachiral materials and metamaterials. First, a linear microstructural model for the free undamped dynamics of the periodic cell is formulated. Second, a Multi-Parameter Perturbation Method (MPPM) is used to achieve an analytical, although approximate, solution for the linear eigenproblem governing the free wave propagation along a generic direction of the cellular material, according to the Floquet-Bloch theory. Different technical issues concerning the location of the unperturbed points in the parameter space, the dimension of the perturbation vector, the occurrence of coalescent frequencies (internal resonances), the accuracy of the asymptotic approximation, the suitability of a certain parameter ordering are discussed. Conclusive remarks are pointed out, with focus on the inertial resonator role in the parametric design of pass/stop bands.

2. Microstructural model

The tetrachiral material is characterized by a regular tessellation of periodic square cells covering the bi-dimensional infinite domain (Figure 1a). The repetitive structure of the elementary cell, or *microstructure*, is composed by a circular ring and four tangent ligaments organized according to a chiral topology (Figure 1b). By virtue of the chiral inter-ring connection, the cellular geometry determines a characteristic *rolling up* deformation mechanism, responsible for the peculiar auxetic behaviour connoting the anisotropic macroscopic response of the material [5–8].

Each massive and highly-stiff ring (with diameter D), is modeled as a rigid body (with mass M and rotational inertia J), possessing three planar *active* degrees-of-freedom collected in the displacement vector \mathbf{q}_1 . The light and flexible ligaments are described by linear, extensible, unshearable and massless beams (with extensional EA and flexural rigidity EI). The natural length of the beams is $L = H \cos \beta$, where H is the cell side length and $\beta = \arcsin(D/H)$ is the ligament inclination angle with respect to the mesh lines connecting the ring centres. Owing to the periodicity, the cell boundary crosses the ligament midspans, which host four configuration nodes possessing three planar *passive* degrees-of-freedom collected in the displacement vectors \mathbf{q}_i ($i = 2..5$). An inertial tetrachiral metamaterial can be obtained by adding local inertial resonators consisting in intra-ring massive inclusions embedded in an annular elastic matrix. Each resonator is modeled as a simple undamped oscillator (with mass M_r , rotational inertia J_r and circular frequencies Ω_r and Ω_θ), possessing three planar *active* degrees-of-freedom collected in the displacement vector \mathbf{q}_6 .

Introducing a certain circular frequency Ω_c as known dimensional reference, a suited minimal set \mathbf{p} of independent nondimensional parameters, sufficient to describe the geometric, elastic and inertial properties of the model, is

$$\delta = \frac{D}{H}, \quad \varrho^2 = \frac{I}{AL^2}, \quad \chi^2 = \frac{J}{MH^2}, \quad \omega_c^2 = \frac{EA}{MH\Omega_c^2}, \quad \gamma = \frac{\Omega_r}{\omega_c\Omega_c}, \quad \alpha^2 = \frac{M_r}{M}, \quad \gamma_\theta = \frac{\Omega_\theta}{\omega_c\Omega_c}, \quad \chi_r^2 = \frac{J_r}{M_rH^2} \quad (1)$$

where δ expresses the spatial density of the rings, measuring also the material mass density. The inverse of ϱ accounts for the beam slenderness. The χ^2 -parameter describes the rotational-to-translational mass ratio of the rings, while ω_c is a nondimensional normalization frequency, assumed to be unitary in the following. The metamaterial design is governed by the key-parameters α^2 and γ , expressing the ring-resonator *mass ratio* and *frequency tuning*.

Seeking for a synthetic but representative alternative to the diffuse but computationally demanding finite element formulations [6, 9], the direct stiffness method can be employed for the parametric formulation of a simple Lagrangian beam lattice model (Figure 1c). Accordingly, the free undamped dynamics of the periodic cell is governed by a linear system of nondimensional ordinary differential equations, defined in the full configuration vector $\mathbf{q} = (\mathbf{q}_1, \dots, \mathbf{q}_6)$. The model dimension can be reduced, without any further approximation, by virtue of a quasistatic condensation procedure applied to the *passive* nodes lying on the cell boundary. Moreover, the Floquet-Bloch boundary conditions can be imposed, in order to account for the free propagation across adjacent cells of planar waves with nondimensional wavevector $\mathbf{b} = (\beta_1, \beta_2)$ where $\beta_1 = k_1 H$ and $\beta_2 = k_2 H$, while k_1 and k_2 are the wavenumbers of the horizontally and vertically propagating waves, respectively. Finally, the free undamped wave dynamics of the periodic metamaterial is governed by a linear equation defined in the reduced configuration vector $\mathbf{q}_a = (\mathbf{q}_1, \mathbf{q}_6)$

$$\mathbf{M}(\mathbf{p})\ddot{\mathbf{q}}_a + \mathbf{K}(\mathbf{p}, \mathbf{b})\mathbf{q}_a = \mathbf{0} \tag{2}$$

where dot indicates differentiation with respect to the nondimensional time $\tau = \Omega_c t$. The Hermitian matrices $\mathbf{M}(\mathbf{p})$ and $\mathbf{K}(\mathbf{p}, \mathbf{b})$ are related to the mass and stiffness of the periodic cell and are reported in details in [3, 10]. In particular, recalling the components of the reduced configuration vector, the equation of motion can be partitioned

$$\begin{bmatrix} \mathbf{M}_1(\mathbf{p}) & \mathbf{O} \\ \mathbf{O} & \mathbf{M}_6(\mathbf{p}) \end{bmatrix} \begin{pmatrix} \ddot{\mathbf{q}}_1 \\ \ddot{\mathbf{q}}_6 \end{pmatrix} + \begin{bmatrix} \mathbf{K}_1(\mathbf{p}, \mathbf{b}) + \mathbf{K}_6(\mathbf{p}) & -\mathbf{K}_6(\mathbf{p}) \\ -\mathbf{K}_6(\mathbf{p}) & \mathbf{K}_6(\mathbf{p}) \end{bmatrix} \begin{pmatrix} \mathbf{q}_1 \\ \mathbf{q}_6 \end{pmatrix} = \begin{pmatrix} \mathbf{0} \\ \mathbf{0} \end{pmatrix} \tag{3}$$

where \mathbf{M}_1 and \mathbf{K}_1 are the mass and (condensed) stiffness matrix of the tetrachiral material, while \mathbf{M}_6 and \mathbf{K}_6 are the mass and stiffness matrix of the resonator. The first row for $\mathbf{K}_6 = \mathbf{O}$ governs the model in the absence of resonators.

3. Band structure of the tetrachiral material

Focusing first on the tetrachiral material, the unknown dimensional Ω and nondimensional frequency $\omega = \Omega/\Omega_c$ can be introduced. Therefore, imposing the harmonic solution $\mathbf{q}_1 = \boldsymbol{\psi}_1 \exp(i\omega\tau)$ in the first row of the equation (3) and eliminating the dependence on time, the in-plane wave propagation is governed by the linear eigenproblem

$$(\mathbf{K}_1(\mathbf{p}, \mathbf{b}) - \lambda\mathbf{M}_1(\mathbf{p}))\boldsymbol{\psi}_1 = \mathbf{0} \tag{4}$$

in the unknown eigenvalue $\lambda = \omega^2$ and eigenvector $\boldsymbol{\psi}_1$. The eigensolution is composed by three eigenvalues $\lambda_h(\mathbf{p}, \mathbf{b})$, satisfying the characteristic equation $F(\lambda, \mathbf{p}, \mathbf{b}) = 0$, and the corresponding eigenvectors $\boldsymbol{\psi}_h(\mathbf{p}, \mathbf{b})$ representing the polarization mode of the ω_h -monofrequent propagating wave. The exact dispersion curves $\omega_h(\mathbf{b})$ along the boundary of the first irreducible Brillouin zone \mathcal{B}_1 are represented by the red lines in Figure 2 for two different parameter sets.

Following a Multi-Parameter Perturbation Method (MPPM) [11–14], the dispersion curves can be asymptotically approximated by defining the extended parameter vector $\boldsymbol{\mu} = (\mathbf{p}, \mathbf{b})$ and introducing the ϵ -power series expansions

$$\boldsymbol{\mu}(\epsilon) = \boldsymbol{\mu}^\circ + \epsilon\boldsymbol{\mu}', \quad \lambda(\epsilon) = \lambda^\circ + \epsilon\lambda' + \epsilon^2\lambda'' + \epsilon^3\lambda''' + \epsilon^4\lambda'''' + \dots \tag{5}$$

where the auxiliary parameter $\epsilon \ll 1$. The approximation holds locally in the neighborhood of the reference parameter set $\boldsymbol{\mu}^\circ = (\mathbf{p}^\circ, \mathbf{b}^\circ)$, for a generic multiparameter perturbation $\boldsymbol{\mu}' = (\mathbf{p}', \mathbf{b}')$. Introducing the parameter ordering $\boldsymbol{\mu}(\epsilon)$ and the eigenvalue expansion $\lambda(\epsilon)$, the ϵ -series approximation of the characteristic function $G(\epsilon) = F(\lambda(\epsilon), \boldsymbol{\mu}(\epsilon))$ reads

$$G(\epsilon) = G^\circ + \epsilon G' + \epsilon^2 \frac{G''}{2!} + \epsilon^3 \frac{G'''}{3!} + \epsilon^4 \frac{G''''}{4!} + \dots + \epsilon^n \frac{G^{(n)}}{n!} + \dots, \quad \text{with } G^{(n)} = \sum_{S_0(h,k)} \sum_{|p|=k} \frac{n! \mathbf{F}^{(h,|p|)}}{(h+k)!} \left[\mathbf{r}_{hp}^{[n]} \right]_{\lambda^\circ \Rightarrow \mathbf{0}} \tag{6}$$

where the (h, k) -index set $S(h, k) = \{h, k \in [0, h+k=n]\}$ and $S_0(h, k) = S(h, k) - (0, 0)$. Defining ℓ the dimension of the parameter vector $\boldsymbol{\mu} = (\mu_1, \dots, \mu_\ell)$ and $a_{jhpn} = j(h+|p|+1) - n$, the partial derivatives for generic h, k read

$$\mathbf{F}^{(h,|p|)} = \frac{\partial^h}{\partial \lambda^h} \frac{\partial^{|p|}}{\partial \mu_{p_1} \dots \partial \mu_{p_k}} F(\lambda, \mu_{p_1}, \dots, \mu_{p_k}), \quad \mathbf{r}_{hp}^{[n]} = \sum_{j=1}^n \left(\frac{a_{jhpn}}{n} \right) \left(\frac{\lambda^{(j)}}{\lambda^\circ} + \sum_{i=1}^{\ell} \frac{\mu_i^{(j)}}{\mu_i^\circ} \right) \mathbf{r}_{hp}^{[n-j]} \tag{7}$$

with initialization $\mathbf{r}_{hp}^{[0]} = (\lambda^\circ)^h (\boldsymbol{\mu}^\circ)^p$. Adopting the \mathcal{B}_1 -vertices as reference $\mathbf{b}^\circ = (\beta_1^\circ, \beta_2^\circ)$ and the parameter ordering

$$\beta_1 = \beta_1^\circ + \epsilon\beta_1', \quad \beta_2 = \beta_2^\circ + \epsilon\beta_2', \quad \delta = \epsilon\delta', \quad \varrho = \epsilon\varrho', \quad \chi = \epsilon\chi' \tag{8}$$

the forth-order approximate dispersion curves are represented by the black circles in Figure 2.

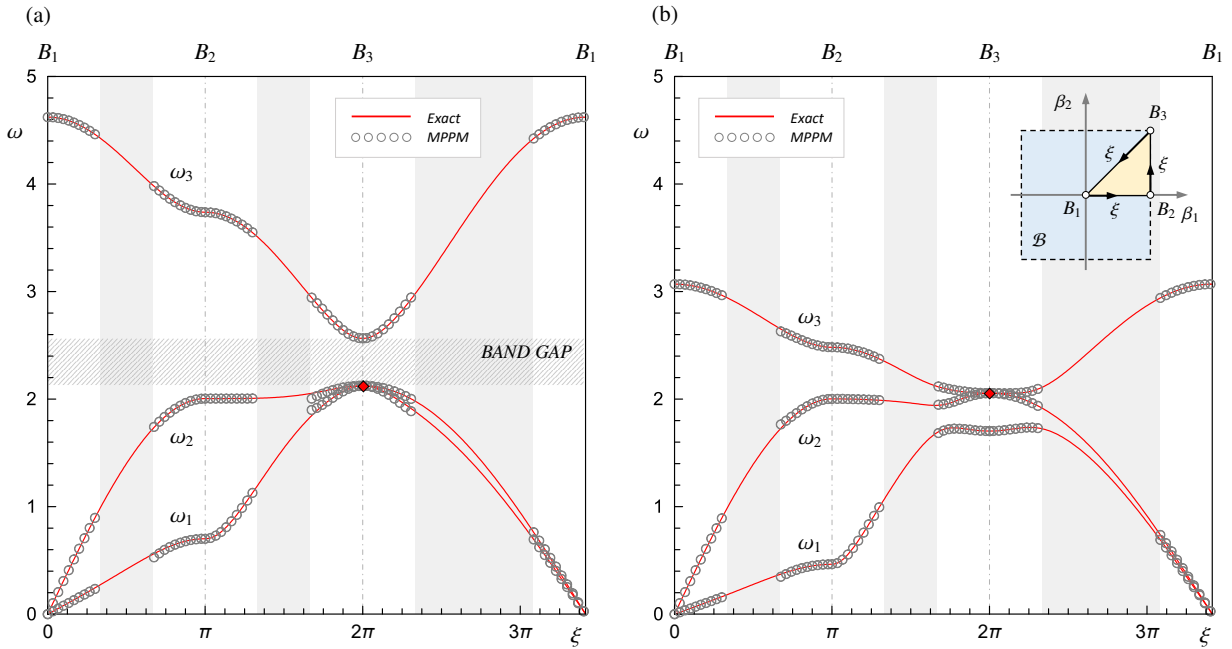


Fig. 2. Floquet-Bloch spectrum of the tetrachiral material. Comparison between the exact and MPPM-approximate dispersion curves for (a) high-density, low-slenderness material $(\delta, \rho, \chi) = (1/10, 1/10, 1/9)$; (b) low-density, high-slenderness material $(\delta, \rho, \chi) = (1/15, 1/15, 1/9)$.

For both the parameter sets, the asymptotic approximation presents a satisfying accuracy for large \mathbf{b} -ranges centered in the \mathcal{B}_1 -vertices (say $|\mathbf{b}'| \leq 1$, or even more). The good approximation accuracy persists also in the internal resonance (or nearly-resonance) regions rising up from couples of coincident (double) eigenvalues in the generating (zeroth-order) solution, where a strong parameter sensitivity is expected (e.g. in B_1, B_3 for $\mathbf{b}^\circ = (0, 0)$ and $\mathbf{b}^\circ = (\pi, \pi)$). Additional reference points could be added to cover the entire Brillouin boundary, properly matching the adjacent local solutions through suited weighting functions, if necessary. As a matter of theoretical and practical interest for the spectrum design and customization, the asymptotically approximate dispersion curves furnish also an analytical parametric assessment for the amplitude of the band gap between the acoustic and optical branches, if it exists.

4. Band structure of the tetrachiral metamaterial

Similarly to the tetrachiral material, the oscillatory solution $\mathbf{q}_a = \boldsymbol{\psi} \exp(i\omega\tau)$ can be imposed in the equation of motion of the tetrachiral metamaterial. Therefore the in-plane wave propagation is governed by the linear eigenproblem

$$(\mathbf{K}(\mathbf{p}, \mathbf{b}) - \lambda\mathbf{M}(\mathbf{p}))\boldsymbol{\psi} = \mathbf{0}, \tag{9}$$

in the unknown eigenvalue $\lambda = \omega^2$ and eigenvector $\boldsymbol{\psi}$. The solution is composed by six eigenpairs $\lambda_h(\mathbf{p}, \mathbf{b}), \boldsymbol{\psi}_h(\mathbf{p}, \mathbf{b})$. The exact dispersion curves $\omega_h(\mathbf{b})$ are represented by the blue lines in Figure 3a, where the tetrachiral material spectrum is marked by red dashed lines. The comparison shows how the inertial resonators enrich the material spectrum and open new band-gaps ($BG_{1,3}$) centered at the frequencies pointed by the tuning parameters γ and γ_θ .

The multi-parameter perturbation method can be easily extended to the metamaterial eigenproblem, by introducing one or the other of the following schemes for the resonator parameter ordering

- Ordering \mathcal{O}_1 (heavy resonators) : $\alpha = \epsilon\alpha', \quad \gamma = \gamma^\circ + \epsilon\sigma, \quad \chi_r = \epsilon\chi_r', \quad \gamma_\theta = \gamma_\theta^\circ$ (10)

- Ordering \mathcal{O}_2 (light resonators) : $\alpha = \epsilon^2\alpha', \quad \gamma = \gamma^\circ + \epsilon^2\sigma, \quad \chi_r = \epsilon\chi_r', \quad \gamma_\theta = \gamma_\theta^\circ$ (11)

without any need of mathematical re-formulation, but taking some algorithmic care about the doubling of the internal resonance conditions. Employing the ordering \mathcal{O}_1 (under the condition $\gamma_\theta^\circ - \gamma^\circ = \mathcal{O}(1)$), the fourth-order local approximation of the lowest dispersion curves for $\mathbf{b}^\circ = (\pi, \pi)$ and $\gamma^\circ = 2$ is marked by the circles in Figure 2b.

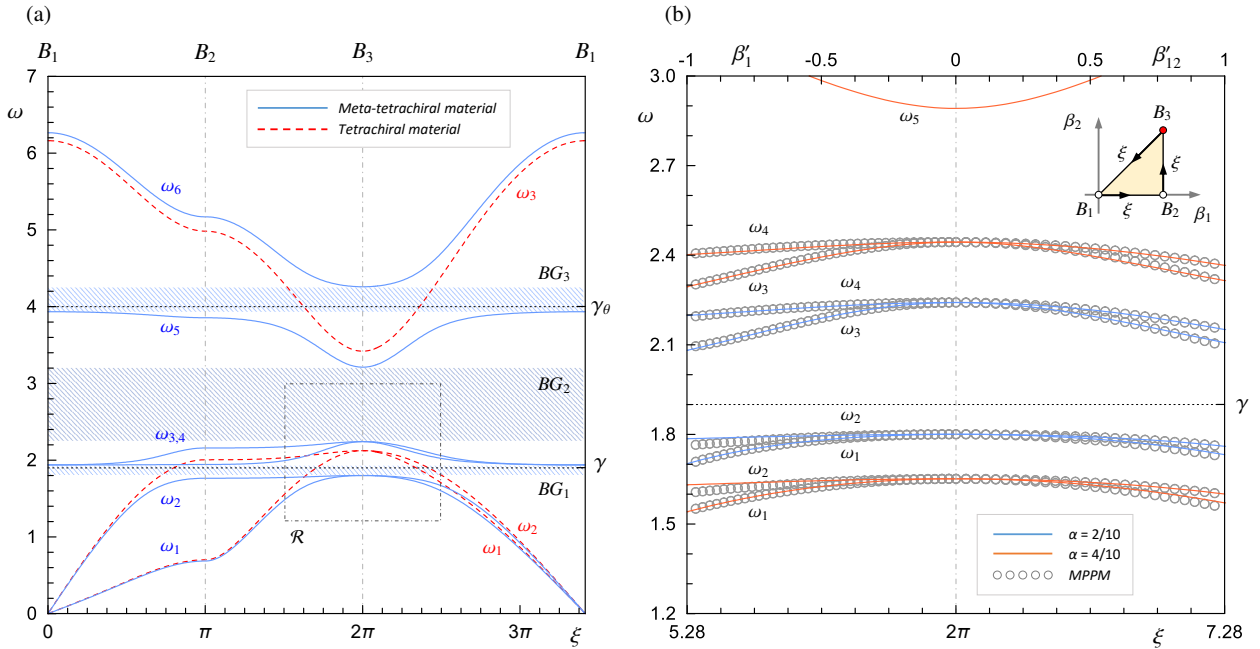


Fig. 3. Floquet-Bloch spectrum of the meta-tetrachiral materials with microstructural parameters $(\delta, \varrho, \chi) = (1/10, 1/10, 1/12)$ and resonator parameters $(\alpha, \gamma, \chi_r, \gamma_\theta) = (2/10, 19/20, 1/11, 4)$: (a) comparison with the spectrum of the tetrachiral material, (b) local MPPM-approximation of the dispersion curves corresponding to the cluster of four close frequencies in the \mathcal{R} -region for different (heavy) resonator ($\alpha = 2/10, 4/10$).

The comparison between the exact and approximate curves demonstrates that the Multi-Parameter Perturbation Method succeeds in treating the enlarged parameter space required to describe the enriched microstructure of inertial metamaterials, featured by the linear ring-resonator coupling. In particular, the approximation accuracy persists even if the multiplicity of the generating (zeroth-order) eigensolution is doubled (up to four coincident eigenvalues) by a perfect tuning of the resonator frequencies (with the σ -perturbation acting as detuning). Figures 4 and 5 show the frequency loci (two pairs of coincident frequencies) in the resonator (α^2, γ) -parameter space for $\mathbf{b} = (\pi, \pi)$. The higher accuracy of the O_1 -ordering (blue loci) for large (α^2, σ) -values can be appreciated (Figures 4). In contrast, the superior efficacy of the O_2 -ordering (green loci) must be remarked for small (α^2, σ) -values, which determine the O_1 -ordering approximation to completely lose validity due to some singularities in the asymptotic functions (Figures 5).

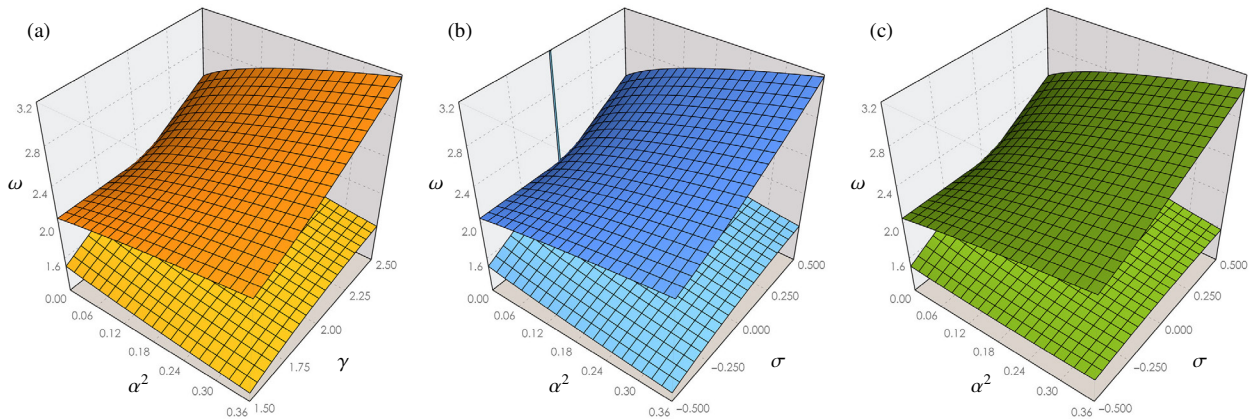


Fig. 4. Frequency loci vs the mass and tuning parameters of the heavy resonator for the meta-tetrachiral material with $(\delta, \varrho, \chi) = (1/10, 1/15, 1/12)$: (a) exact, (b) MPPM-approximation according to the O_1 -ordering, (c) MPPM-approximation according to the O_2 -ordering.

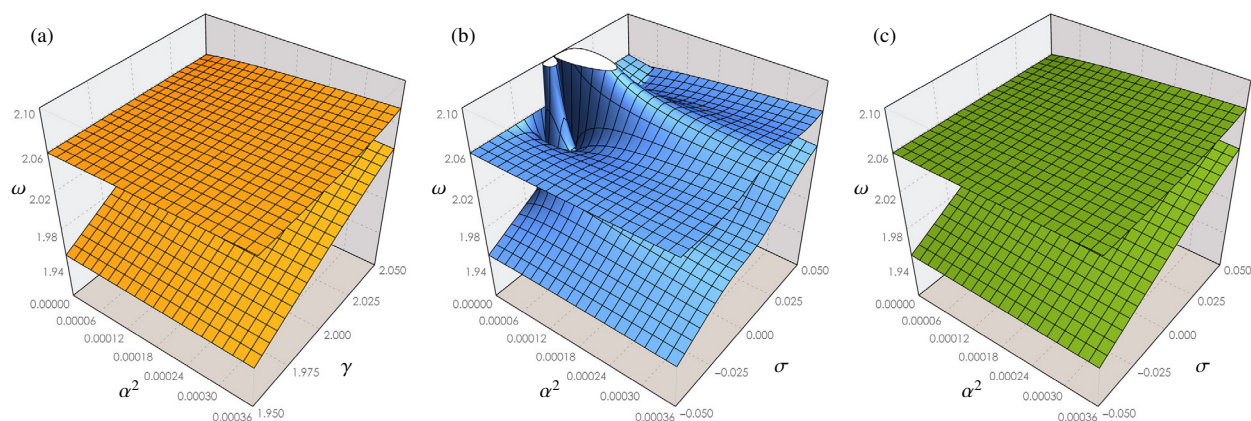


Fig. 5. Frequency loci vs the mass and tuning parameters of the *light* resonator for the meta-tetrachiral material with $(\delta, \varrho, \chi) = (1/10, 1/15, 1/12)$: (a) exact, (b) MPPM-approximation according to the O_1 -ordering, (c) MPPM-approximation according to the O_2 -ordering.

5. Conclusions

A parametric beam lattice model has been formulated for the free propagation of linear elastic planar waves in periodic tetrachiral materials and metamaterials. By virtue of multiparametric perturbation techniques, an analytical asymptotic approximation has been achieved for the dispersion functions in the whole Brillouin zone. The approximation accuracy demonstrates that perturbation methods succeed in dealing with the large parameter space required to characterize the rich microstructure of inertial metamaterials. Consequently, a multi-parametric, perturbation-based, analytical description can be pursued for the dispersion spectrum of the metamaterial, featured by a dense structure of pass and stop bands determined by internal resonance or nearly resonance conditions.

References

- [1] A. Bacigalupo, Second-order homogenization of periodic materials based on asymptotic approximation of the strain energy: formulation and validity limits, *Meccanica* 49 (2014) 1407–1425.
- [2] A. Bacigalupo, M. Lepidi, G. Gnecco, L. Gambarotta, Optimal design of auxetic hexachiral metamaterials with local resonators, *Smart Materials and Structures* 25 (2016) 054 009.
- [3] A. Bacigalupo, L. Gambarotta, Simplified modelling of chiral lattice materials with local resonators, *International Journal of Solids and Structures* 83 (2016) 126–141.
- [4] A. Bacigalupo, G. Gnecco, M. Lepidi, L. Gambarotta, Optimal design of low-frequency band gaps in anti-tetrachiral lattice meta-materials, *Composites Part B* 115 (2017) 341–359.
- [5] J. N. Grima, R. Gatt, P.-S. Farrugia, On the properties of auxetic meta-tetrachiral structures, *physica status solidi (b)* 245 (2008) 511–520.
- [6] A. Alderson, K. Alderson, D. Attard, K. Evans, R. Gatt, J. Grima, W. Miller, N. Ravirala, C. Smith, K. Zied, Elastic constants of 3-, 4- and 6-connected chiral and anti-chiral honeycombs subject to uniaxial in-plane loading, *Composites Science and Technology* 70 (2010) 1042–1048.
- [7] Y. Chen, X. N. Liu, G. K. Hu, Q. P. Sun, Q. S. Zheng, Micropolar continuum modelling of bi-dimensional tetrachiral lattices, *Proceedings of the Royal Society of London A: Mathematical, Physical and Engineering Sciences* 470 (2014) 1–17.
- [8] A. Bacigalupo, L. Gambarotta, Homogenization of periodic hexa- and tetrachiral cellular solids, *Composite Structures* 116 (2014) 461–476.
- [9] K. Tee, A. Spadoni, F. Scarpa, M. Ruzzene, Wave propagation in auxetic tetrachiral honeycombs, *Journal of Vibration and Acoustics* 132 (2010) 031 007.
- [10] A. Bacigalupo, G. Gnecco, M. Lepidi, L. Gambarotta, *Design of Acoustic Metamaterials Through Nonlinear Programming*, Springer International Publishing, Cham, 2016, pp. 170–181, doi: 10.1007/978-3-319-51469-7_14.
- [11] A. Luongo, F. Romeo, A transfer-matrix-perturbation approach to the dynamics of chains of nonlinear sliding beams, *Journal of Vibration and Acoustics* 128 (2006) 190–196.
- [12] M. Lepidi, Multi-parameter perturbation methods for the eigensolution sensitivity analysis of nearly-resonant non-defective multi-degree-of-freedom systems, *Journal of Sound and Vibration* 332 (2013) 1011–1032.
- [13] M. Lepidi, V. Gattulli, A parametric multi-body section model for modal interactions of cable-supported bridges, *Journal of Sound and Vibration* 333 (2014) 4579–4596.
- [14] A. Bacigalupo, M. Lepidi, High-frequency parametric approximation of the floquet-bloch spectrum for anti-tetrachiral materials, *International Journal of Solids and Structures* 97-98 (2016) 575–592.